THE TOPOGRAPHIC CHANGE MECHANISM OF CORAL CAYS

Kenya Takahashi[1], Hiroyuki Katayama[1], Yudai Iwatsuka[1], Tsunehiro Sekimoto[1], Takuya Suzuki[2], Hajime Kayanne[2] and Masahiko Isobe[3]

Coral cays are low-lying islands formed by the gravel from coral reefs, which build up to a position slightly higher than the sea level. In past research, coral cays were reported to have formed and been disappeared by short-term high waves. The mechanisms of their destruction are uncertain, however, because of the difficulty in obtaining observation data. In this study, we investigated the topographic change mechanisms of coral cays by a laboratory model experiment and field surveys on Barasu Island, located near the north side of the Iriomote Island During the course of the study, topographic changes in sediment deposition, erosion, and movement repeatedly occurred due to the strong external forces of typhoons. The direction of sediment movement at Barasu Island qualitatively agreed with the direction of the observed external force. Moreover, although the external force was erosive in one direction, when the external force originated from two directions, the Barasu Island area expanded.

Keywords: coral reef, coral cays, wave observation, model experiment, steep-slope reef, gravel transport

INTRODUCTION

Coral cays are low-lying islands formed by the gravel from coral reefs, which builds up to a position slightly higher than the sea level. They are often seen in the Pacific and Indian Oceans' island nations, and are more than 200 in number. Understanding the formation and maintenance mechanisms of these coral cays will help in the conservation of not only the Japanese islands but also the Pacific Ocean island nations that are threatened by global warming.

Past studies have reported that coral cays are formed and disappeared by short-term high waves. Well-known examples include the storm ridge in the southeast portion of Funafuti Atoll in Tuvalu formed by tropical cyclone "Bebe" (Uda 2013), and Udahafushi Island of North Male in Maldives in the Indian Ocean (Uda 1988). However, their formation mechanisms are not quantitatively understood because wave observation data is yet to be acquired during the terrain change process. While hydraulic model experiments on the formation mechanism of coral cays have been conducted (Takahashi et al. 2011 and Uda et al. 1990, 1992, 1995), they have used only 2-dimensional model experiments. Hence, while the formation mechanism of coral cays is qualitatively understood from previous studies, a quantitative understanding of their formation and maintenance processes is yet to be achieved.

In this study, we investigated the topographic change mechanisms by conducting a laboratory model experiment and field surveys of the Barasu Island, located near the north side of Iriomote Island in Japan.

Figure 1. Photos of typical coral cays (Funafuti and Barasu Island).

[1] Institute of Technology, Penta-Ocean Construction Co. Ltd., 1534-1,Yonku-cho, Nasu-shiobara, Tochigi, 329-2746, Japan
[2] Department of Earth and Planetary Science, The University of Tokyo,7-3-1, Hongo Bunkyo-ku, Tokyo, 113-0033, Japan
[3] Kochi University of Technology, Tosayamada, Kami-city, Kochi, 782-8502, Japan

FIELD SURVEY ON THE BARASU ISLAND

Our survey site is the Barasu Island, located north of the Iriomote Island, Yaeyama region, Okinawa, as shown in Figure 2. The Barasu Island is nearly in the center of a flat oval reef measuring about 0.3 km on the short axis and about 1 km on the long axis. Its entire circumference is surrounded by a steep-slope with a gradient of about 1/30. Since this reef is shielded in the southern and northern directions by the Iriomote Island and Hatoma Island, respectively, we considered external forces to be limited to those from the east and west directions.

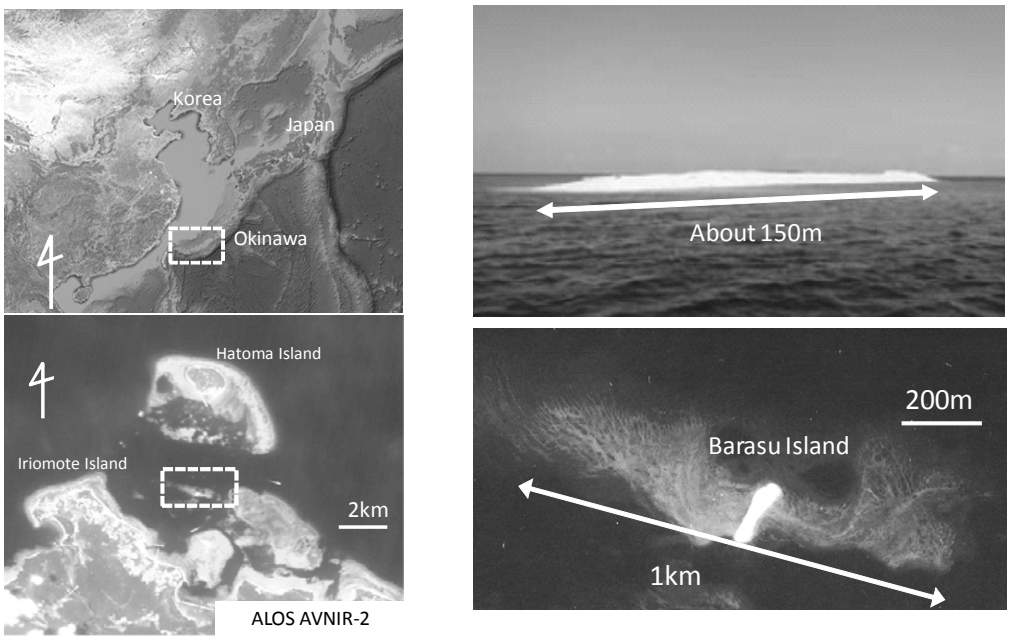

Figure 2. Location of Barasu Island.

Figure 3 shows wave frequency distributions, divided according to wave directions in the open sea 5 km north of Hatoma Island. Wave height and wave direction data are taken from Grid Point Value (CWM) data provided from the Japan Meteorological Agency. At this location, the prevailing wind direction is north–northeast during the autumn–winter monsoon season. During spring–summer, this location experiences a large number of typhoons passing through. This location infrequently experiences significant wave heights of more than 3 m in the east–southeast direction during typhoons.

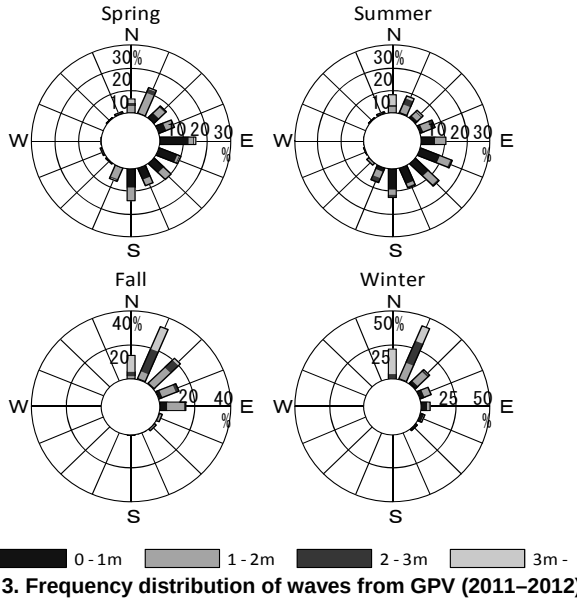

Figure 3. Frequency distribution of waves from GPV (2011–2012).

Wave Observation Method

To study the topographic change mechanisms at the Barasu Island, we conducted field observations of wave height and flow velocity at points inside and outside the reef surrounding the Barasu Island. Figure 4 shows the observation points of wave height and flow velocity from July to October, 2012, which was also the middle of the typhoon season. We continuously observed water levels, pressure, and two components of flow velocity at 0.5 s sampling intervals. All observation data were grouped into data sets of 20 min for the purposes of statistical processing. As shown in the figure, W600 and E600 were installed at about 10 m water depth (Mean Sea Level criteria) near the reef edge, and W200 and E200 were installed at about 3 m water depth on the reef flat.

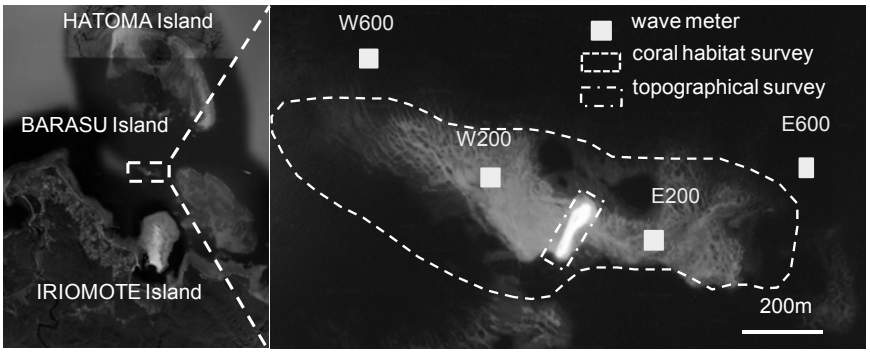

Figure 4. Equipment placement for wave observation.

Wave Observation Results

Typhoons passed by the Iriomote Island 7 times during this observation period (Figure 5), and observations were made of the topographic changes to the Barasu Island before and after the passage of each typhoon. We first assumed that the movement of the Barasu Island due to the typhoon was in qualitative agreement with the direction of the flow velocity on the reef. We further supposed that deposition would take place on the reef if the flows from both east and west occur, and erosion would occur if the flow originated from either direction.

To clarify the presence of a causal relation between deep flow and topographic changes, we created a UV plot of the flow velocity and direction, as shown in Figures 7(a) and 7(b). Figure 7(a) shows a plot of the flow velocity for the period 9:40–10:00 on August 11 during the passage of typhoon No. 9. The waves measured at this time showed a maximum height of significant waves at E200 to be about 1.5 m, but the maximum height of significant waves at W200 was as low as about 1.0 m. It is clear, even with respect to the UV plot, that compared with the west side, the flow velocity change was larger on the east side. This analysis shows that topographic change resulting from typhoon No. 9 was caused by external forces from the east. Similarly, the UV plot of the flow velocity during the passage of typhoon No. 11 is shown in Figure 7(b). For this typhoon, the significant wave height on the west side of the Barasu Island was larger than that on the east side, with the same tendency in the average flow velocity and UV plot as well. We presume that the external force from the west side moved the Barasu Island eastward.

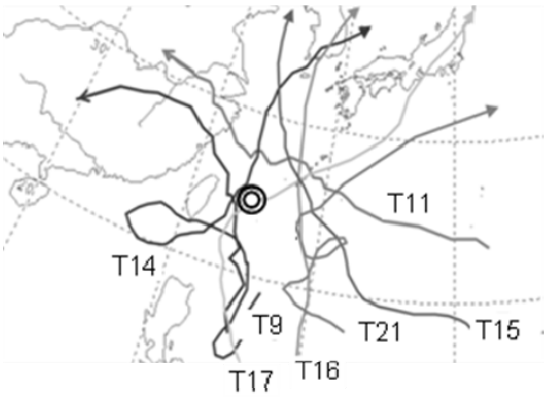

Figure 5. Routes of typhoons in 2012.

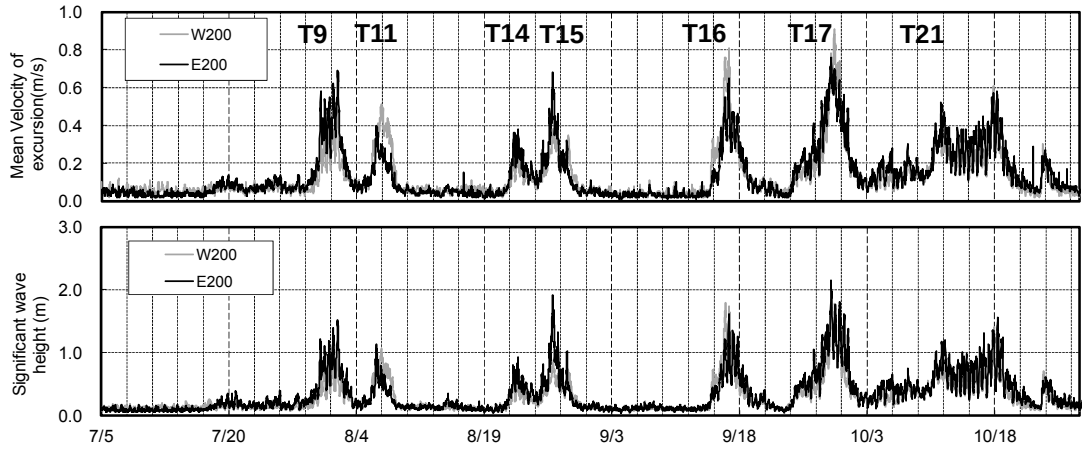

Figure 6. Wave observation results.

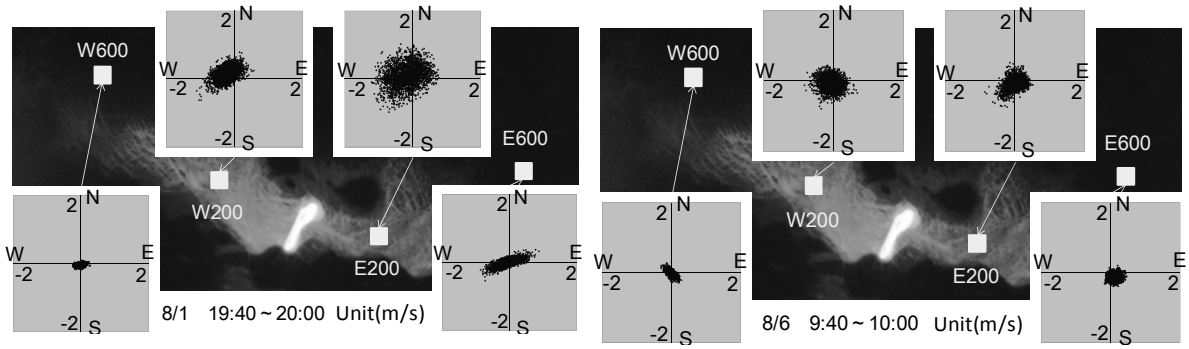

(a) Typhoon 9 **(b) Typhoon 11**

Figure 7. UV Plot of Flow Velocity.

LABORATORY MODEL EXPERIMENT

Our experimental model was a 3-dimensional wave flume with a reflected wave absorption control function (length: 20 m, width: 30 m, depth: 1.2 m). We used a steep-slope reef model with a fixed bed around the open ocean that simulated a typical coral reef island (reef flat: long axis: 5 m, short axis: 2 m, height: 0.7 m, slope: 1/5 gradient around entire circumference, experimental scale: 1/100) (Figure 8). The reef surface comprised coarse finished mortar to simulate the roughness of patchy coral. The underlying reef material comprised silica sand, about 0.61 mm in diameter, assuming the local coral gravel.

The experiment was conducted for nine cases, as shown in Table 1, with variations in wave conditions, water depth on the reef flat, and the underlying thickness of the sand layer. We considered cases with high waves as those experiencing typhoons (Cases 1–5), and cases with waves typically found in the ocean at this location (Cases 6–9). In addition, the conditions of Case 9 include a one-way irregular wave so that the control case (Case 1) and the total wave energy are equal. The significant wave specifications are shown in Table 1.

In the experiment, after wave action for 15 min, we conducted a superficial topographic survey using an ultrasonic range finder. Furthermore, we checked for any topographic change with respect to the types of wave action generated, for waves generated within 60 min. After 60 min had passed, if a balanced topographic state had not been reached, waves were generated for up to a maximum of 180 min. After 60 and 120 min, we conducted a topographic survey, and evaluated the amount of sediment movement.

Regarding the waves and the flow of incident wave conditions on the reef, we first used a fixed-bed model experiment without sand. In this fixed-bed experiment, we installed 21 wave gauges and 8 electromagnetic current meters, and we measured the water level and the flow velocity at a 20-Hz sampling frequencies. In the movable bed model experiment, all reef measuring instruments were removed so that when we generated the waves, the movement of the sediments would not be blocked.

Figure 8. Photo of the laboratory model experiment.

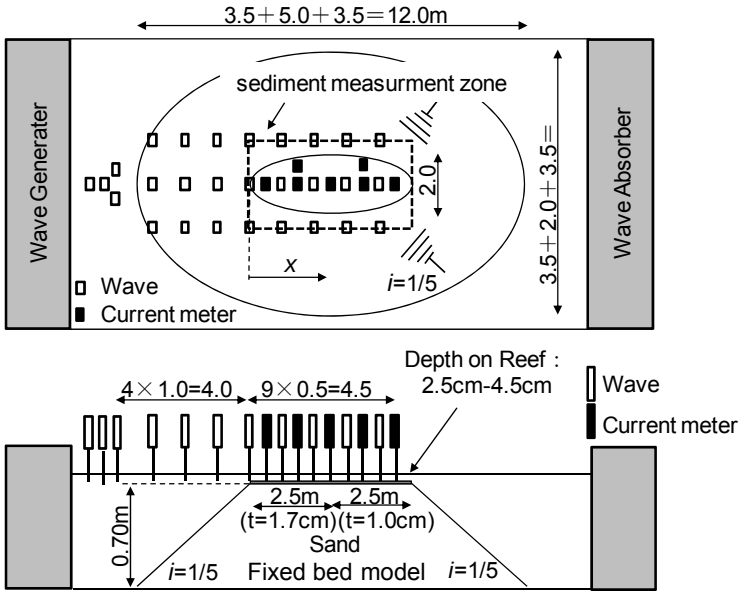

Figure 9. Equipment placement in the laboratory model experiment.

Table 1. Experiment parameters for nine cases in the 3D model.					
Case		Wave Height (cm)	Wave Period (s)	Water Depth (cm)	Remarks
1	High Waves	3.6	1.2	3.5	Basic Case
2		3.6	0.9	3.5	Short Period
3		3.6	1.2	2.5	Low Water Level
4		3.6	1.2	4.5	High Water Level
5		5.6	1.6	3.5	High Wave Height
6	Normal Waves	1.8	0.8	2.5	Basic Case
7		1.8	0.8	3.5	Mean Sea Level
8		1.8	1.2	2.5	Long Period
9		2.5	0.8	2.5	Uni-directional Random Wave

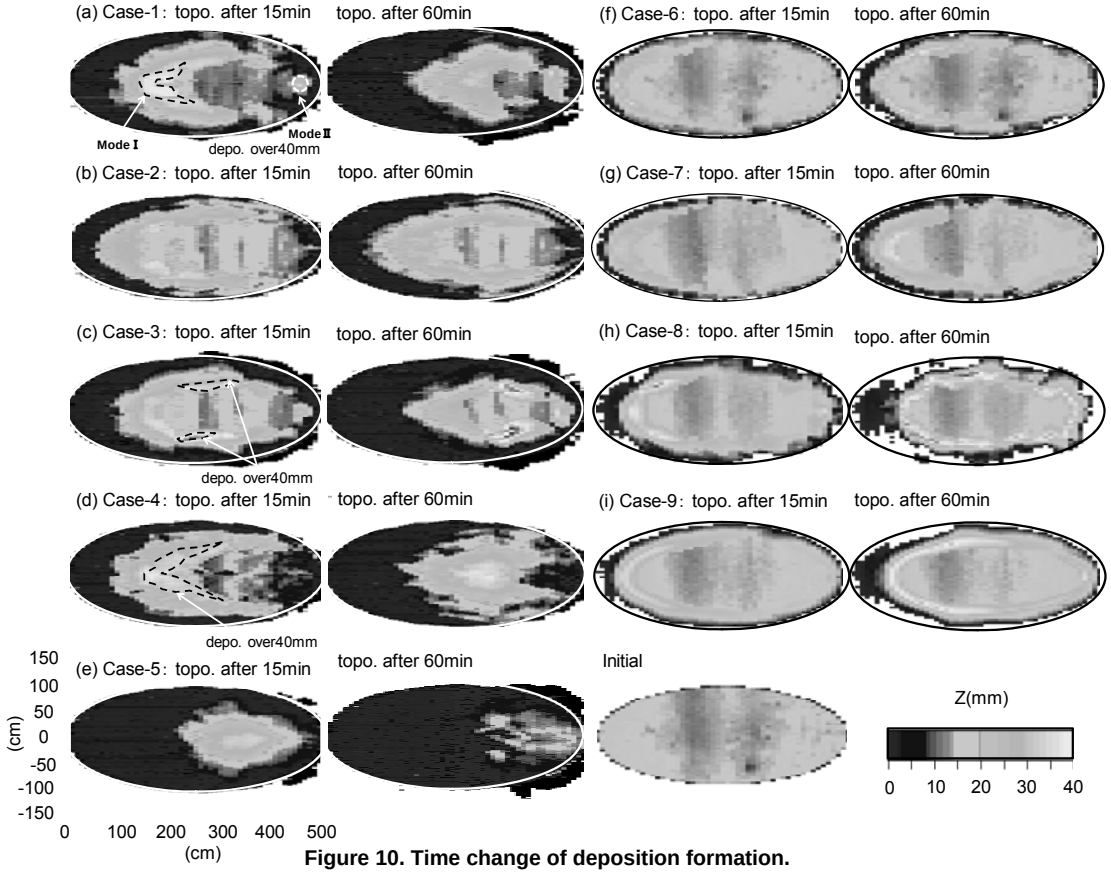

Figure 10. Time change of deposition formation.

Figure 10 shows the deposition of sediments during the experiment. After 15 min of wave generation, in Cases 1 and 3, a deposition appeared with a deposition height of the water surface. Deposition regions included Mode 1, which appeared in the reef center, and Mode 2, which appeared at the back of the reef, as shown in the figure. The deposition of Mode 2 is considered to have been formed by the influence of diffraction waves on the reef. Its position was related to the reef length axis and the diffraction waves from the reef edge, which met at a focal point away from the sides of the reef. While sediment formation is an unstable process, it is a phenomenon that is greatly influenced by not only the waves and flow but also the formation of the reef itself. Therefore, we next consider the results of the Mode 1 deposition.

In all the high wave cases, the Cs values (parameter of Sunamura (1984)) were greater than 18 (erosion form). Although the deposition appeared temporary over mean sea level, in time, the deposition moved to the back of the reef and was eroded.

Although big differences in the deposition pattern were not seen in Cases 3 and 4, whose water depths were different from that in Case 1, the maximum deposition height increased with the water

depth in Cases 3 and 4, and sediments appeared over mean sea level. The height at this time roughly agreed with the average water level from the wave setup during the fixed-bed experiment.

The deposition quantity increased at high tide due to the big wave setup, and experiments have also reproduced this result, as reported by Uda (1988) and Takahashi et al. (2011). Similarly for Case 5, wherein only the water depth was changed, when wave height was higher than in the basic case, the tractive wave force increased. As a result, the amount of sediment movement also increased, and almost all sediments eroded away after waves had been generated for 60 min.

Figure 11(a) shows the movement of sediments after 15–120 min of wave generation in Case 1, which shows the basic high waves case. Although a temporary deposition formed in the central reef area during the movement process, it retreated under the influence of breaking waves caused by the strong reef edge with time. Figure 11(b) shows the movement of sediments after 15–180 min of wave generation in Case 6, which shows the basic normal waves case. After 15 min, a ring-like deposition formed and was connected to a position about 50 cm from the front reef edge. And the top of this deposition appeared above the water. After 15 min of wave generation, there was little deposition movement from the center to the back of the reef. As time passed, the ring-like deposition expanded, and its connection with the reef became nearly complete after 120 min. Although the deposition position near the reef edge slowly retreated, it continued to expand up to the 180 min limit. In these conditions, the influence of a diffraction wave peculiar to the coral reef island was in effect. The influence of wave breaking at the reef edge was small, because the wave height and period were small. In other words, the wavelength decreased in comparison with the reef size, resulting in the formation of the ring-like deposition.

Moreover, in Case 7 (with a deep water depth) and Case 8 (with long period waves), we see a retreat of the deposition position at the reef edge. In Case 9 (irregular wave case), the deposition position at the reef edge retreated very little, and the deposition width was stable. Here, we consider that the high waves not only caused a tractive force effect but also had the effect of causing the steep-slope of the reef front deposition.

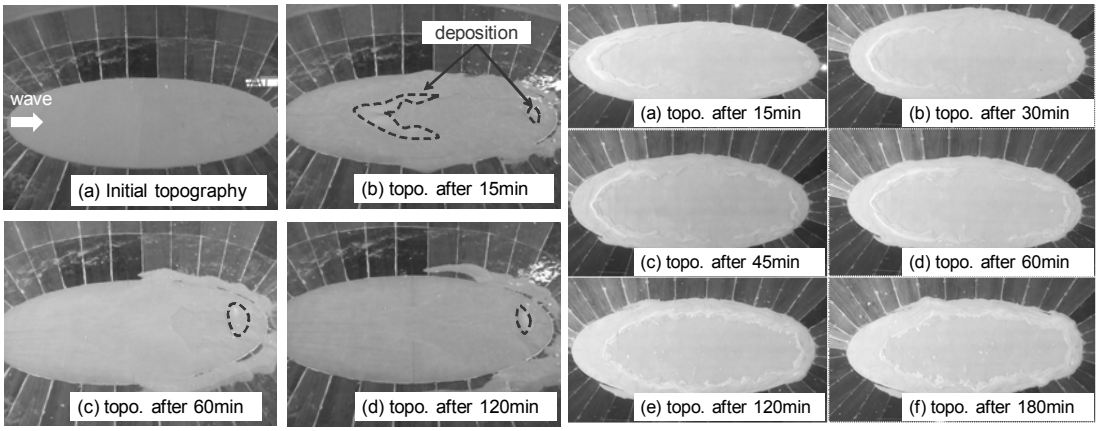

Figure 11. Sedimentary mechanism of coral cays.

Figure 12 shows vertical cross sections of the topographic changes on the long axis of the reef center during the experiment. The wave setup surface in this figure is the value at the time of the fixed-bed experiment. This figure shows that the external force action of waves and the flow into the reef resulted in it being covered with a ring-like deposition. No topographic changes occurred within the reef; movement of sediments occurred only near the reef edge. Moreover, our research shows that the height of the average increase in the water level is small for the reefs surrounded by open oceans.

With respect to variations per hour, Cases 7, 8, and 9 show that the deposition positions retreated more than in Case 6. With respect to the amount of change from the initial sand position, deposition height almost stayed the same. However, in Case 8 (with long period waves), the sediments near the reef edge were eroded the most, and as long as there was no supply of sediments, there was no further expansion of the deposition topography.

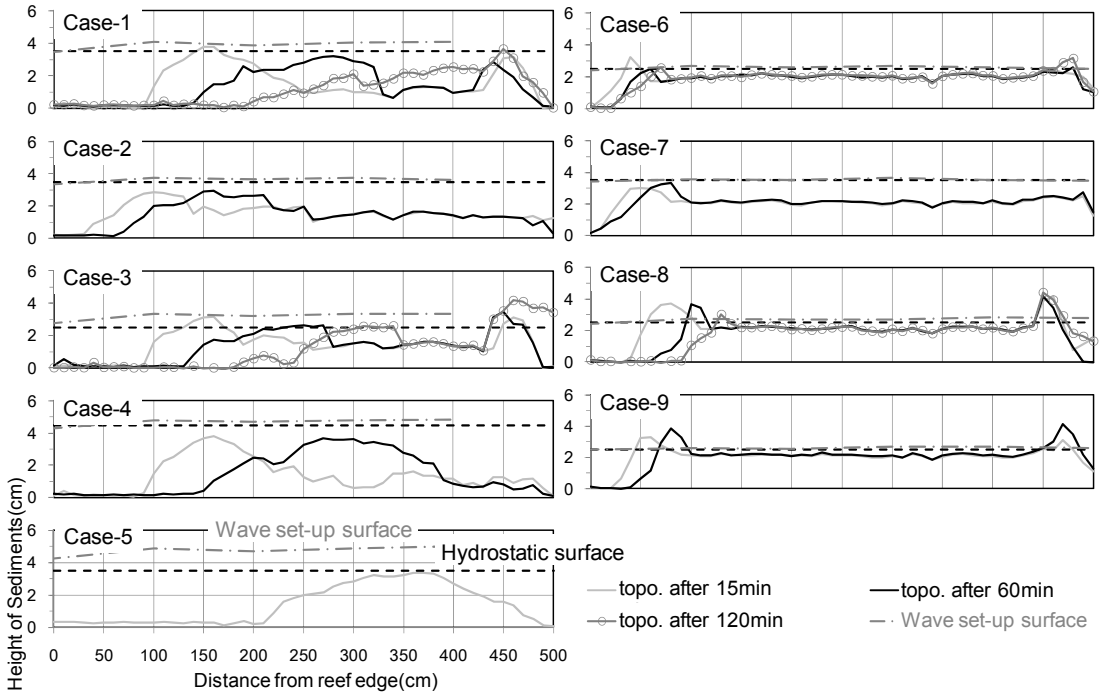

Figure 12. Vertical sections of topographic change in 9 cases.

Figures 13(a) and 13(c) show the root mean square wave height, and Figures 13(b) and 13(d) show the mean flow velocity along the reef length axis. Although the root mean square wave height temporarily increased with the incident wave height near the reef edge, it was caused by wave-breaking attenuation near the reef edge and the difference in every case was small over the reef. However, as shown in Cases 1, 3, and 5, incident wave heights were large and the mean flow velocity increased so quickly that there was almost uniform distribution over the reef. Moreover, in Cases 6, 8, and 9 with normal waves, all the flow velocities on the reef were 0.25 m/s or less, and the tractive force on the reef was declining. From this effect, although there was some movement of sediments at the reef edge, compared with the high waves' cases, the movement of sediments within the reef was insignificant.

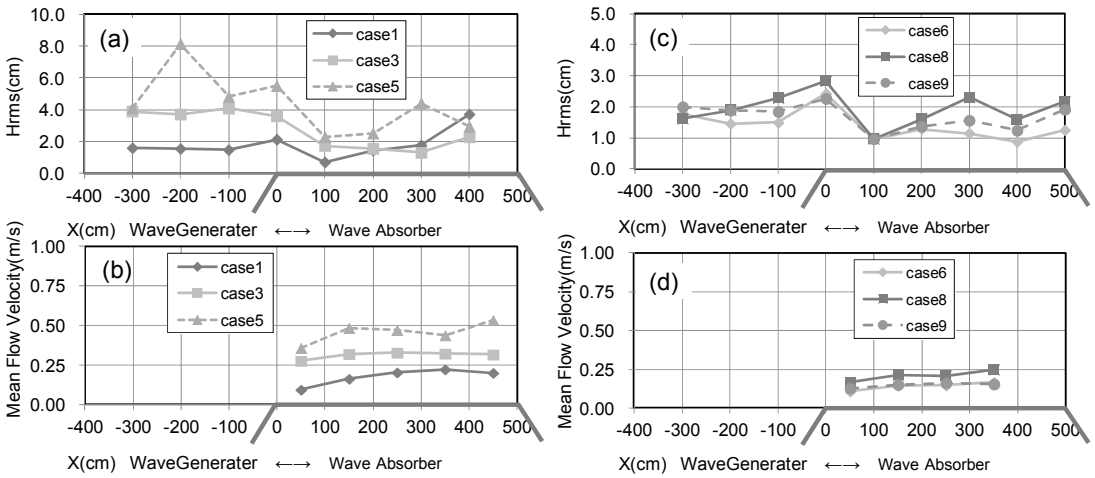

Figure 13. Wave height on the reef, and distribution of flow velocity.

Figure 14 shows a mimetic diagram of the formation mechanism of deposition. In Cases 1–5 with high waves, although there was a case showing deposition in two modes, fundamentally the external force action increased. Some erosion tendencies were shown as time progressed. In this case, although the wave period compared to reef length was comparatively long, the influence of the refraction and diffraction characteristics in open-type reefs was small.

On the other hand, in Cases 6–9, although the external force action and the motion of sediments were small, since the wave period was short, the influence of refraction and diffraction over the reef influence was apparent. We consider that the external force on the reef center from the entire reef circumference had expanded.

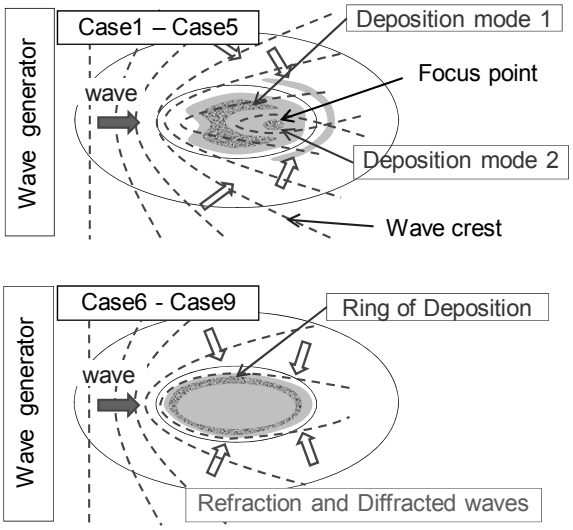

Figure 14. Sedimentary mechanism on coral cays.

CONCLUSIONS

Using a field survey and three-dimensional hydraulic model experiment, we confirmed that the movement of sediments is caused by the waves and flow on the reef, and our study results are summarized as follows:

1. Repetitive topographic changes in deposition, erosion, and movement by the strong external force of a typhoon were caused mainly by the flow.
2. Wave breaking at the reef edge, caused by the effect of the open ocean and the surrounding steep-slope reef, formed a ring-like deposition, and by the shielding effect this deposition was maintained and its topography expanded.
3. The relative relation between wavelength and reef size are important in the formation and maintenance processes of coral cays on reefs.
4. The appearance of sediment deposition, deposition formation, and deposition position are greatly influenced by the flow velocity on the reef.

Our future research objectives include the quantitative evaluation of coral cays formation conditions and the establishment of a numerical forecasting model.

REFERENCES

Iwatsuka, Y., H. Katayama, T. Sekimoto, K. Aoki, H. Kayanne, and M. Isobe. 2012. Study on formation mechanism of coral cays on a steep slope reef. *Proceedings of Coastal Engineering (B2)*, JSCE, 68 (2), 476-480.

Kayanne, H. 2011. A coral reef and coral cays ecotechnological preservation and creation - Ecotechnological preservation and creation technology of an island which a living thing builds -, C*ivil Engineering Technology*. 66 (11), 53-58.

Sunamura, T. 1984. Quantitative predictions of beach face slopes, *Geological Society of America Bulletin*, 95, 242-245.

Suzuki, T., H. Kayanne, Y. Iwatsuka, H. Katayama, T. Sekimoto, and M. Isobe. 2013. Studies on the topographic change mechanism of coral cays. *Proceedings of Ocean Engineering (B3)*, JSCE, 69 (2), 838-843.

Takahashi, K., H. Katayama, T., Sekimoto, K. Aoki, and M. Isobe, 2011. Influence of waves, currents and gravel supplies on the formation of coral cays, *Proceedings of Coastal Engineering (B2)*, JSCE, 67 (2), 636-640.

Uda, T. 1988. The field survey of the storm surge disaster in the Maldive Islands. *Proceedings of Coastal Engineering*, JSCE, 35 (2), 212-216.

Uda, T., S. Tanimoto and A. Sakano and T. Takagi. 1990. The move mechanism of the piece of coral in a reef top and the reef gap circumference, *Proceedings of Coastal Engineering*, JSCE, 37 (2), 215-219.

Uda, T., S. Kosuga. H. Ito, and J. Yamazaki. 1992. Research on formation and disappearance mechanism of coral, *Proceedings of Coastal Engineering*, JSCE, 39 (2), 376-380.

Uda, T., S. Kosuga, and M. Suzuki. 1995. Experimental research about the formation mechanism of coral cays, *Proceedings of Ocean Engineering*, JSCE, 11 (2), 73-78.

Uda, T., S. Onaka, and T. San-nami. 2013. Field observation of deposition of gravel to Funamanu Island in Tuvalu due to tropical cyclone bebe, *Proceedings of Ocean Engineering (B3)*, JSCE, 69 (2), 820-825.